# ASTARTE-4B Response in COVA IT/10 Experimental Test Simulation by Different Internal Structure Schematization

A. Daneri, G. Sordon, G. Toselli
*ENEA, CRE "E. Clementel", Via Mazzini 2, I-41038 Bologna, Italy*

Abstract

In this paper a study executed by ASTARTE-4B /1/, /2/ is presented to evaluate how different models adopted in the schematization of fast breeder reactor internal structures affect the explosive phenomenon simulation during an HCDA.

Reference is made to the COVA series experimental model IT/10 /3/. In some previous calculations the internal structure was treated as rigid and firm /4/, /5/. In two new series of calculations in which either a part or the whole structure has been treated by elastic-plastic model, shock wave propagation across the structure is taken into account. These calculations have been carried out thanks to opportune code modifications /2/. The results obtained compared with the experimental ones, have shown a more correct reproduction of shock wave transmission.

## 1. Introduction

The aim of the work described is the lagrangian code ASTARTE-4B /1/, /2/ response analysis in the simulation of models having thick inner structures. For this study experimental model IT/10 /3/, of the COVA series was considered. The internal structure in the model was formerly treated as rigid and firm (/4/ and /5/).

Two calculations, in which part or all the internal structure has been treated with elastic-perfectly plastic model, are presented and the results compared with the experience and results of one of the previous calculations /5/.

The two calculations considered have been realized after a code modification /2/ which permits adoption of a slide line between fluid and elastic-plastic material. It was thus possible to properly represent the fluid sliding along the internal wall of the cylindrical part of the internal structure.

Besides, the elastic-plastic representation of the structure permits good shock wave transmission across the structure. However, in the second calculation there were problems regarding system energy balance. To overcome this it was necessary to use a smaller time-integration step and introduce a suitable rotational damping term /6/ at the slide line points.

## 2. IT/10 experimental model

The IT/10 test /4/ consists of a rigid undeformable cylindrical tank (700 mm inner diameter, 560 mm height) with rigid and undeformable roof and base (circular plates). The tank contains water to a height of 535 mm with a 25 mm cover air at atmospheric pressure under the roof. Inside the tank there is an inner thick steel structure: a coaxial cylinder (23.5 mm thick, 264 mm inner diameter, 360 mm height) open above and closed below by a 40 mm thick diagrid plate. The top of the diagrid is at a height of 100 mm; this is connected to the base by a perforated rigid support.

The explosive charge (L.D.E.) is a sphere (204 $cm^3$ volume and 55.08 g weight) with center on the symmetry axis at a height of 22 mm.

## 3. IT/10 calculation models

Different schematizations have been adopted for the internal tank to simulate the IT/10 model.

A first model has been made considering this tank as rigid and firm and a detailed analysis of the results is reported in /5/.

Subsequently, two further series of calculations have been executed: in these, as already mentioned, part or all the internal tank has been treated by elastic-perfectly plastic material model.

In all calculations the components, except the internal structure, have been represented in the same way. The equations of state adopted (for the fluid, Mie Grüneisen equation, explosive, JWL equation, cover gas, adiabatic equation) are the same as those used in /4/ and /5/.

The adopted lagrangian mesh presents slight differences in the three calculations owing to the different treatment of the internal tank. A spheric representation with 8 meshes for explosive charge has been chosen, taking into account the conclusion reported in /5/.

### 3.1. IT/10.R: rigid internal tank

As a reference calculation with rigid internal tank, one of the test cases analysed in /5/ (IT/10.B, here named IT/10.R) was chosen. The fluid has been assumed as sliding along the cylindrical internal wall of the tank. In fig. 1 the initial lagrangian mesh (18 lines K x 28 lines L) is shown. Lines K=7 and 8 are respectively the "master" and "slave" lines of the "slide" line between fluid and structure.

### 3.2. IT/10.EP1: cylindrical part of the internal tank treated with the elastic-perfectly plastic material model

The IT/10.EP1 test is characterized by modelling the cylindrical internal tank according to the elastic-plastic material theory. The horizontal plate is still rigid and firm.

The EP1 calculation has been performed after introducing a modification described in /2/ into ASTARTE-4B. This modification allows the adoption of a slide line when an elastic-plastic material faces one of the slide line boundaries. We note that without this possibility the fluid movement simulation is not realistic and abnormal mesh distortions, which may stop calculation, arise.

Fig. 2 shows the initial lagrangian mesh (19 K-lines x 28 L-lines). The slide line is

defined, too, by lines K=7 and K=8. The elastic-perfectly plastic material is defined as follows:

equation of state, $p = E\,(\rho - \rho_o)/3\,(1-2\nu)$ $_o$
$P_{min} = -Y_o/3$, $\rho_o = 7900$ kg/m$^3$, $\nu = 1/3$ (Poisson's coefficient),
$E = 1.93 \times 10^{11}$ Pa (Young modulus) and $Y_o = 5.136 \times 10^8$ Pa (Yield stress).

These characteristics have been obtained by approximating the stress-strain law of the material forming the tank, with an elastic-perfectly plastic law so that the integrals of the two stress-strain curves are equal up to a deformation value of 0.2. The material stress-strain law is the same as that used for the internal shell of the IT/12-COVA model /1/.

To avoid excessive "hour glass" distortions, which produce a strong, unphysical increase in elastic-plastic material energy, a pseudoviscosity rotational term (0.05) (except for the mesh points on the slide line) has been introduced.

### 3.3. IT/10.EP2: internal tank treated with elastic-perfectly plastic material model

In the IT/10.EP2 test the whole internal tank has been treated with elastic-plastic material model having the same characteristics as that adopted in the EP1 test.

In some preliminary calculations the lagrangian EP1 schematization was considered. At point A of fig. 2 the firm point condition was adopted, neglecting the support presence. In some calculations some energy balance problems arose: the relative energy increment is greater in the horizontal plate, particularly in the central zone nearest to the symmetry axis. To overcome this we introduced the continuity condition, $(\partial u_z/\partial R)_{R=0}=0$, for elastic-plastic material nodes lying on the axis. In elastic-plastic material treatment it is important to take into account this condition, because stress deviators depend explicitly on velocity gradients.

Fig. 3 shows the mesh grid adopted in the new calculation, IT/10.EP2, in order to better approximate the continuity condition. A rotational pseudoviscosity term (0.1) was applied to a mesh grid band covering the elastic-plastic material (except the mesh points on slide line) and the contiguous zones. The energy balance has considerably improved and the calculation has continued at significant times for phenomenon simulation. Nevertheless at longer times, system energy still increases. This increase seems to depend on the numerical approximations adopted and on slight hour glass distortions still present in grid meshes contiguous to the slide line. A parametric study was made concerning the integration time steps and introduction of the possible use of rotational pseudoviscosity also at slide line points, and then identifying the better parameter choice for good energy balance /6/. However, since the results of physical interest (pressures and impulses on containment), are not very different in any of the calculations, we have reported only IT/10.EP2 here.

## 4. Comparison between calculations and experimental results

### 4.1. Phenomenon chronology

From a global analysis of spatial pressure and velocity distributions three different behaviours of shock wave propagation are evident: in the R calculation the shock wave rises

upwards in the internal tank and then spreads externally and downwards; in EP1 it gets spread also directly across the cylindrical internal tank and then under the bottom; in EP2 it spreads simultaneously in all directions (figs. 4, 5, 6). Consequently the impact on the roof begins at different times: before 600 μsec in R, at 630 μsec in EP1 and 648 μsec in EP2. Finally, while in R test there is no fluid detachment from the roof at final time (2750 μsec), in the other two tests it occurs between 2300-2400 μsec.

### 4.2. Energies, pressures and impulses

From a comparison of the three calculations, one can see that energy behaviours in the different system components does not present essential differences, with the exception, obviously, of the elastic-plastic material. There are some differences, more evident in EP2, as regards total fluid energy (fig. 7) and cover gas energy (fig. 8) due to the treatment of the inner structure. The different cover gas behaviour, from R to EP2, reflects the different phenomenon chronology described above.

For the elastic-plastic material the EP2 case presents excessive energy absorption after 2000 sec, so that the system is no longer conservative. Also in EP1, after this time, an analogous phenomenon is evident, but negligible in amount (the percentage difference between energy absorbed by the system and released by the explosive does not exceed 10%).

As regards the impulse and first pressure peak at the containment bottom there is, for all three calculations, an underestimation, decreasing from R to EP2, which becomes almost zero at the most external bottom points (figs. 9, 10). With respect to the experience, all the calculations show a delay, always less in EP2, of the first pressure peak. All this confirms that the model adopted in EP2 gives a better representation of the phenomenon. What has been said is evident also on the lateral wall, even if EP1 and EP2 results are very similar.

Agreement with the experience is less good in the high part of the vessel, where, after 2000 μsec, there is overestimation of the impulses. The results obtained at the roof are, in general, less satisfactory, although they are coherent with the adopted models. As for the first pressure peak it is recorded at almost the same time as the experience in EP1 and EP2, while it is anticipated in R; however, in all three calculations the peak presents an overestimation which is less in EP2 and becomes zero in the external part of the roof. The impulses, on the contrary, are underestimated in the central and overestimated in the external part, more in EP2. In general, it is possible to observe that the impulse results are less satisfactory in the zone between the roof and the external tank; this is probably due to the lagrangian model of the code.

Finally, as for the internal tank the results are similar in EP1 and EP2: the first pressure peak is underestimated and delayed, while the impulses on the plate are good up to 2000 μsec and overestimated afterwards; on the internal lateral wall they are overestimated, but EP2 results are better.

## 5. Conclusions

What was noticed in the result analysis made in chapter 4, shows the validity and usefulness of the modifications made to the elastic-plastic material treatment of the code

since they permitted phenomenon simulation improvement and enlargement of the code application field.

## 6. References


/1/ Cigarini M., Daneri A., Toselli G., Zucchini A.: "ENEA Version of the Lagrangian code ASTARTE-4. Later Developments and User's Manual Modifications" ENEA-RT/ING (82)24 (1982).

/2/ Daneri A., Sordon G., Toselli G.: "ASTARTE-4B Modifications Made to the Elastic-Plastic Material Treatment and New Rezoning Facility". ENEA RT/TIB/84/10 (1984).

/3/ Verzeletti G., Holtbecker H.: "Report on COVA Firing IT/10/1" EE/92/78 JRC, ISPRA (1978).

/4/ Albertini C. et al.: "The JRC-COVA Programme - Final Report" ER 8705 EN CCGS(83)-CONT-D164 JRC, ISPRA (1983).

/5/ Daneri A., Orefice L., Toselli G., Trombetti T.: "Lagrangian Analysis of Explosive Models with Simple Inner Structures" ENEA-RT/ING (83)4 (1983).

/6/ Daneri A., Toselli G.: "Energy Balance Sensitivity Study by ASTARTE-4B for a Simplified Model with Internal Thick Structures" ENEA RT/TIB/85 (to be published).


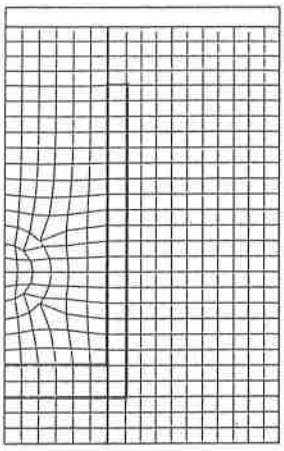

Fig. 1. IT/10.R initial lagrangian mesh.

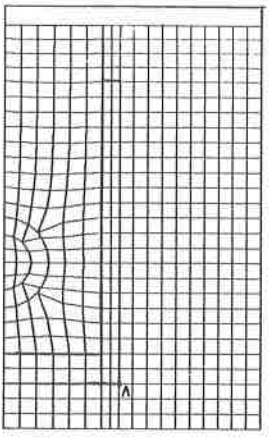

Fig. 2. IT/10.EP1 initial lagrangian mesh.

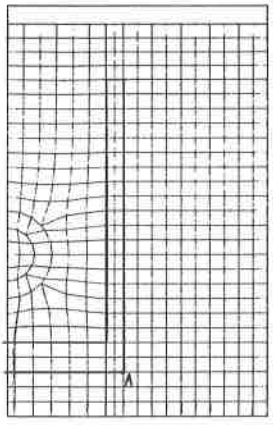

Fig. 3. IT/10/EP2 initial lagrangian mesh.

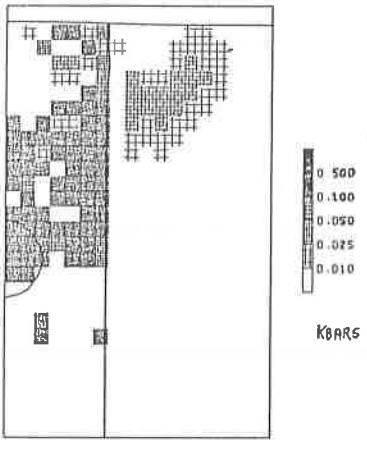


Fig. 4. IT/10.R pressure configuration at 300 μ sec.

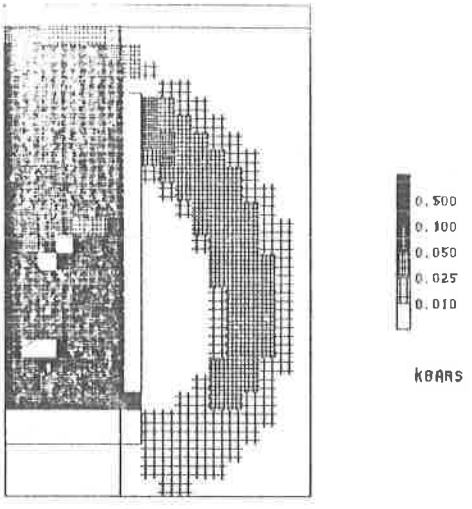


Fig. 5. IT/10.EP1 pressure configuration at 201 μsec.

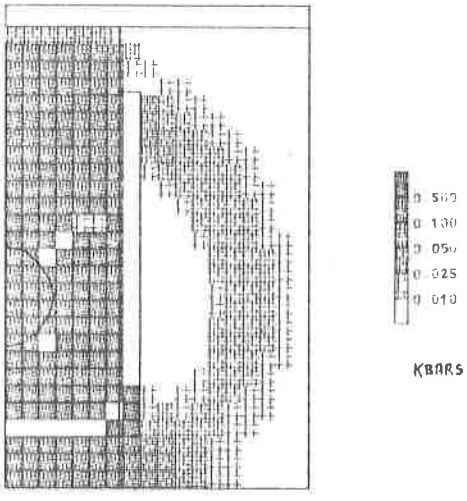


Fig. 6. IT/10.EP2 pressure configuration at 200 μsec.

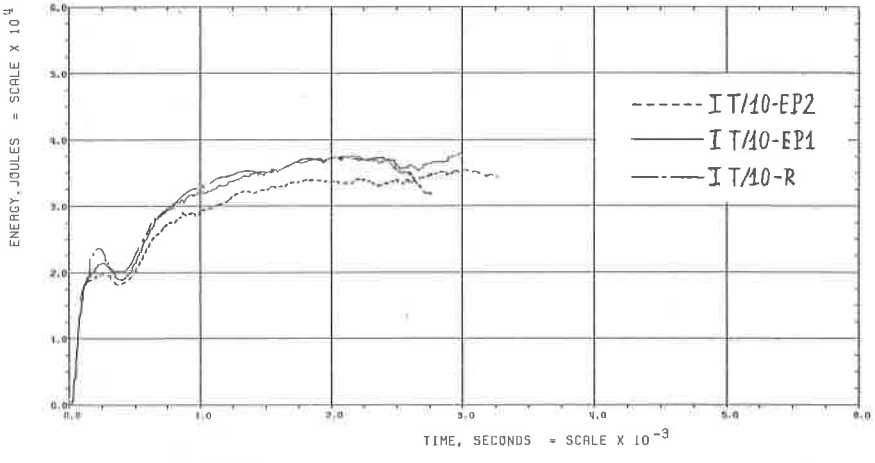


Fig. 7. Total water energy.

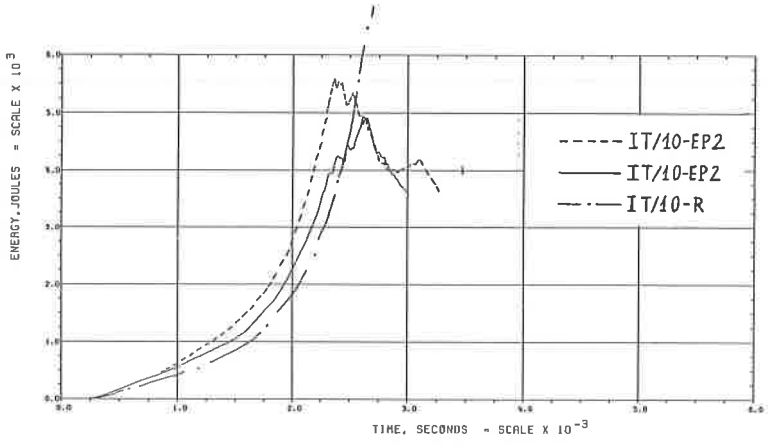


Fig. 8. Internal cover gas energy.

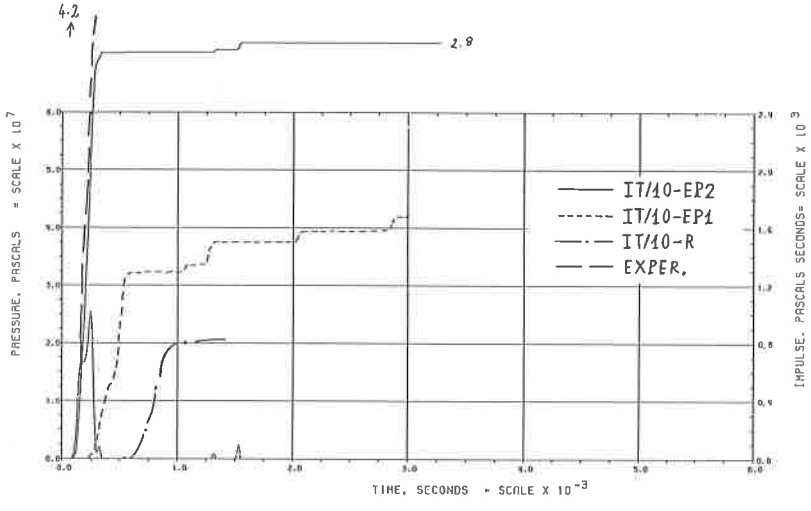


Fig. 9. Pressure and impulses at point R=42 mm, Z=0.

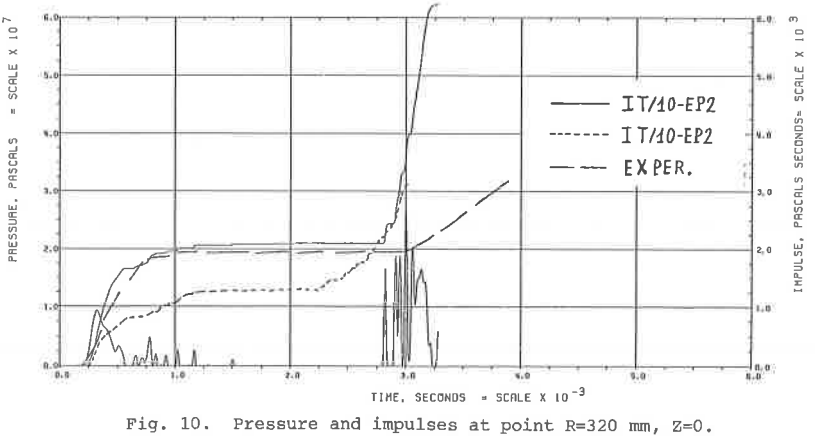


Fig. 10. Pressure and impulses at point R=320 mm, Z=0.